Heat Stress in Human Labor and Poverty: The Case of Ghana

June 2022

Report No: AUS0002918

Ghana

Ghana Green Growth PASA

Heat Stress in Human Labor and Poverty: The Case of Ghana

June 2022

Environment, Natural Resources, and the Blue Economy Global Practice

Acknowledgements

This report was prepared by a team led by Kanta Kumari Rigaud and Neeta Hooda. The team was composed of Wajiha Saeed, Thomas Hertel, Qinqin Kong and Matthew Huber, all of Purdue University.

The team is grateful for the inputs and comments received from Stephane Hallegate, Andrew Burns, Aurelien Kruse, Sheu Salieu, Hugo Alexander Rojas Romagosa, Paul Andres Corral Rodas, Lorenzo Carrera, Brian James Walsh and Sally Beth Murray that helped to improve the report.

Team acknowledges the overall guidance received from Sanjay Srivastava (Practice Manager) and Simeon Ehui (Regional Director, West and Central Africa).

The team would also like to acknowledge the generous support provided for preparation of the report by the Global Program on Sustainability, administered by the World Bank.

Contents

Acronyms

BLS	U.S. Bureau of Labor Statistics
CMIP6	6th Coupled Model Intercomparison Projects
GBP	Gross Domestic Product
GLSS	Ghana Livings Standard Survey
GTAP	Global Trade Analysis Project
HH	household
ILO	International Labor Organization
ORS	Occupational Requirements Survey (of the BLS)
RCP	Representative Concentration Pathway
SSP	Shared Socioeconomic Pathway
WBGT	Wet Bulb Globe Temperature
WDI	World Development Indicators

1 Introduction

In this paper, we assess the economic impacts of increased heat stress in humans in Ghana. As mean global temperatures increase, human capacity for manual labor is affected, particularly in activities with sun exposure such as agriculture and construction. This aspect of climate change is not well-studied, but, as this report will show, this is an important omission, particularly in regions where (i) heat and humidity are already high, (ii) there is high reliance on outdoor, manual labor, and (iii) a significant portion of the population is poor. The effects of heat stress and the resulting losses of labor capacity in such regions can cause large losses of output and GDP. These losses are likely to occur unevenly, affecting certain areas and economic sectors more than others. Some types of poor households (HH) are also likely to be disproportionately affected, especially those close to the poverty line if they earn large portions of their income from their labor and own few productive assets.

We present projections of heat stress and labor capacity losses at high spatial resolution to identify the areas within Ghana that are most at risk. We then assess the economic impacts for 65 different sectors of the economy. We can therefore identify, with a high degree of specificity, both the locations and the economic activities that are in danger of experiencing the largest heat stress-induced labor capacity losses, and losses of output and value addition. The poverty impacts of human heat stress in Ghana are also assessed, disaggregated to identify the HH types that are more likely to be pushed into poverty.

2 Methods

The study methodology is summarized here, with a more exhaustive discussion in Annex 1.

2.1 Climate Data and Estimation of Heat Stress

Heat stress refers to conditions in which it is not possible for the human body to regulate internal temperature. This is most likely to occur when high air temperature coincides with high humidity, since this prevents sweat from evaporating and cuts off an important cooling mechanism. Other environmental variables affecting heat stress are solar radiation and wind conditions. These four variables (temperature, humidity, radiation and wind) are used to calculate the Wet Bulb Globe Temperature (WBGT),[1] a metric for the measurement of heat stress. The WBGT is our preferred metric since it incorporates all four ambient factors and has well-established safety thresholds.[2]

This study considers a future scenario in which mean global temperature increases by 3°C relative to the baseline period, 1961-1990. We use Representative Concentration Pathway (RCP) 8.5 from the 6th Coupled Model Intercomparison Projects (CMIP6) to generate projections of the four specified climate variables at 0.25^{o} x 0.25^{o} grid cell-level, for three-hourly intervals. Our estimates of heat stress therefore have a high degree of spatial and temporal precision. The derived values are then scaled to obtain WBGT per °C of global warming.

2.2 Estimation of Labor Capacity Losses

2.2.1 Grid cell labor capacity losses, by work intensity and work conditions

Using the estimates of heat stress represented by the WBGT, we assess likely labor capacity losses using a labor response function (Brode, Fiala, Lemke, & Kjellstrom, 2018) that is pegged to the ISO7243 safety standard (ISO, 2017). ISO7243 provides thresholds for WBGT that, when exceeded, necessitate that a fraction of each work hour be spent at rest. These thresholds therefore provide limits for the use of human labor under conditions of heat stress, without risk to health. We can thus estimate labor capacity losses for every grid-cell that are consistent with safe labor use.

Labor capacity losses depend also on the intensity of work (physical exertion) and on whether the work is performed under sunny or shaded conditions.[3] We consider four different work intensities measured in watts of metabolic output. Work under sunny/outdoor conditions entails exposure to solar radiation and wind. For work under shaded conditions, we assume that (a) there is no solar radiation; and (b) wind speed is very low, consistent with indoor movement only. We do not account for air conditioning in indoor work conditions. Our approach only accounts for loss of productivity of

[1] The WBGT is estimated using Liljegren's explicit formulation (Liljegren, 2008).
[2] The WBGT is used in safety standards for athletic, occupational, and military settings.
[3] In implementing the labor response function, assumptions must be made with regards to (i) the intensity of works being performed (metabolic output in terms of MWh), and (ii) whether conditions are sunny or shaded.

physical labor; we are unable to account for the effect of heat stress on cognitive skills and any additional productivity loss that this might bring about.

For every grid cell, this approach generates eight different estimates of labor capacity loss (covering four work intensities in both indoor and outdoor conditions), at three-hourly intervals.

2.2.2 Grid-cell labor capacity losses, by sector and labor-type

For each grid cell, we then translate labor capacity losses for each work intensity in indoor and outdoor conditions into labor capacity losses, by sector and by labor type. To do this, we use data from the U.S. Bureau of Labor Statistics (BLS, 2020). The BLS data provides indicators of work intensity and frequency of outdoor exposure for different types of workers[4] in different sectors. We use these data to obtain capacity losses that are specific to labor types and sectors.

More formally, from the first step (described in section 2.2.1) we obtain $z_{r,g}^{i,c}$: labor capacity losses in grid-cell g of region r, which vary over labor intensities $i = \{200\text{W}, 300\text{W}, 400\text{W}, 600\text{W}\}$ and vary with sunny or shaded condition indicated by index $c = \{sunny, shaded\}$. These are translated to $z_{l,a,r,g}$: labor capacity loss for labor type l in activity/sector a (in grid-cell g of region r):

$$z_{l,a,r,g} = \sum_{c} \sum_{i} z_{r,g}^{i,c} \alpha_{l,a}^{c} \beta_{l,a}^{i}$$

where $\alpha_{l,a}^{c}$ is the sun exposure-related share (the portion of labor type l in activity a exposed to work condition c) and $\beta_{l,a}^{i}$ is the intensity-related share (portion of labor of labor type l in activity a with a work intensity of i). These shares are estimated from the BLS.

The estimated sun exposure share for blue-collar workers in the U.S. using the BLS data is approximately 22%. We adjust the modelling for lower-income countries where a reduced level of mechanization means that the sun exposure of blue-collar workers in agriculture is likely to be much greater than it is in the U.S. We assume that the sun exposure of such workers has a logarithmic relationship with GDP per capita; and that the sun exposure in Malawi is 90% (out of the 137 countries/regions in our model, Malawi has the lowest GDP per capita, therefore we assign it the extreme value). Figure 1 shows the logarithmic curve passing through these two data points and the implied sun exposure in a selection of low-income countries. These adjusted sun exposure shares are used to determine labor capacity losses for blue-collar workers in agriculture in Ghana (and could be used for any other country in the dataset).

[4] We disaggregate labor into four types: blue-collar (low skill workers in agriculture and other low-skill workers), white-collar (office workers), technical and other professionals, and service and shop workers.

Figure 1: Adjusted region-specific sun exposure shares for blue-collar workers $(\alpha_{l,a}^{c})$

Panel A: Assumed relation between sun exposure and GDP per capita

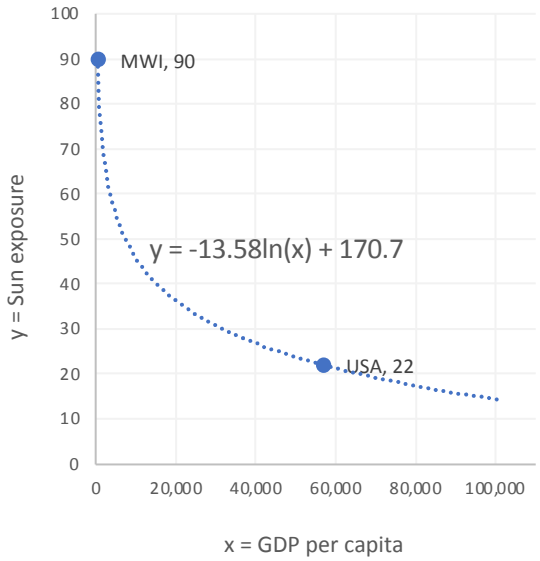

Panel B: Calculated sun exposure for a selection of low-income countries

2.2.3 Region-level labor capacity losses, by sector and labor-type

Since our economic model, described in greater detail in the next section, is not a grid cell-level model, we next need to obtain labor capacity losses at the region level. Thus, we aggregate labor capacity losses over grid-cells using certain assumptions. For non-agricultural sectors, we assume that the spatial distribution of activities corresponds to the spatial distribution of population, so we use each cell's population for weighting. Thus, if very hot grid cells are sparsely populated, they will have less influence on the aggregated estimate of labor capacity loss for manufacturing, services, etc. as a whole. In the case of agriculture, region-level labor capacity losses can be estimated using known agricultural output to weight grid cells. It is assumed that the spatial distribution of agricultural workers is the same as the spatial distribution of agricultural output. These assumptions are outlined in greater detail in Annex 1.

2.3 Economic Framework and the Estimation of Poverty Impacts

2.3.1 Economic framework

Finally, economic impacts are assessed using the income estimation model of the Global Trade Analysis Project (GTAP-POV). As GTAP is a global general equilibrium framework, the modelled economic impacts account for higher order spill-over effects from global trade linkages, sectoral dependencies, competition for factors of production, and the circular flow of income through the global economy. This is critically important for assessing the economic impacts of climate change, as this is a global phenomenon with significant trade impacts. The model uses version 10 of the GTAP

database, with 2014 as the base year, and disaggregates the global economy into 137 countries/regions and 65 sectors.

2.3.2 Estimation of HH incomes at the poverty lines

The -POV extension to the GTAP income model allows for the estimation of changes in the real income of households (HH) that lie close to the poverty line. Price changes (of commodities and factors) determined by the 'macro' model are used as inputs into a 'micro' module, which estimates changes in real incomes of HHs that lie 'in the neighborhood of poverty' (defined as the one decile of HHs encompassing the poverty line). We impose a poverty line in local currency terms that is consistent with the 12.7% poverty rate for Ghana for 2017, as reported in the World Bank's World Development Indicators (WDI) database using the $1.90 per day poverty line.

These poor HHs are disaggregated into seven categories (strata) based on their source of earnings:

- Agricultural HHs, who earn 95% or more of their income from agricultural self-employment,
- Non-agricultural HHs, who earn 95% or more of their income from non-agricultural self-employment,
- Rural labor/Urban labor HHs, who earn 95% or more of their income from wage labor,
- Transfer HHs, who earn 95% or more of their income from transfers, and
- Rural diverse/urban diverse HHs, who do not fall into any of the other strata.

Each HH stratum's earnings are apportioned to different sources: land, capital, and labor, where labor is further separated into: self-employed agricultural skilled and unskilled labor, self-employed non-agricultural skilled and unskilled labor, and wage-earning skilled and unskilled labor. Using HH survey data from Ghana, initial estimates of the shares of each of these factors in total HH earnings are determined, for each stratum. These earnings shares are determined using the most recent Ghana Livings Standard Survey (GLSS 7) (Ghana Statistical Service, 2017), as shown in Panel A of Figure 2. It is noteworthy that the survey base estimates indicate a large share (64.5%) of skilled labor in the earnings of the agricultural stratum.

However, data from the GTAP 10 database, which is based on data from the International Labor Organization (ILO), suggests a different portioning of skilled and unskilled labor's value added in agriculture in Ghana and other countries in West Africa. We therefore make an adjustment to the earnings shares of the agricultural stratum to make them consistent with ILO-based portioning of skilled and unskilled agricultural labor. The result of this adjustment is shown in Panel B of Figure 2.

Figure 2: Earnings shares

A. Shares based on GLSS 2017 survey

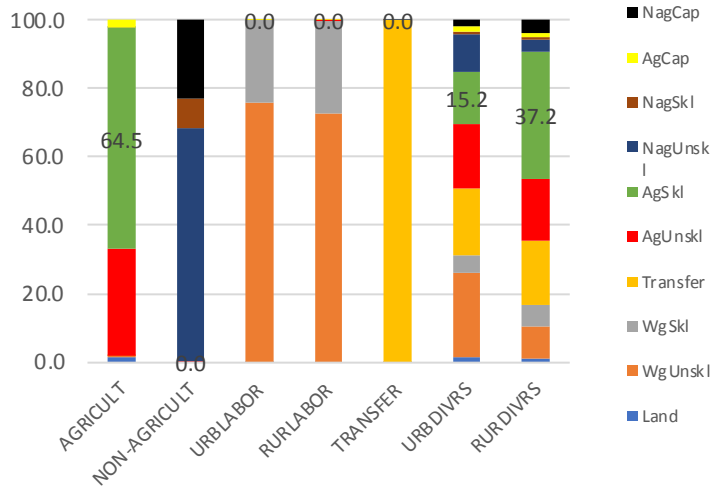

B. ILO-based adjusted shares for agricultural stratum

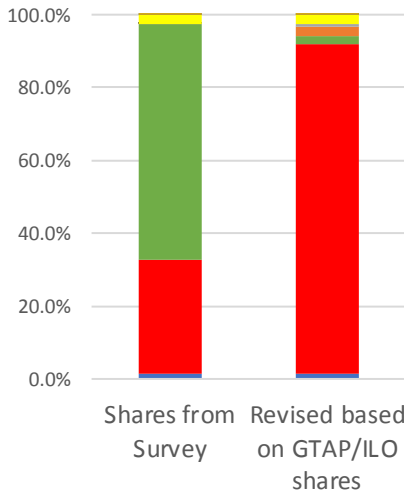

Using these (ILO-adjusted) earnings shares, the income of HHs in stratum s of region r is determined as:

$$Y_{r,s} = \sum_{i} \alpha_{r,s,i} \left(W_{r,s,i} - C_r\right)$$

where $\alpha_{r,s,i}$ are the earnings shares as discussed above and i is the set of factors. $W_{r,s,i}$ is the change in factor $i's$ price (returns to factor i) determined in the main macro model. This is adjusted by the cost of living at the poverty line, C_r, in order to obtain changes in income in real terms. Thus, if there is a large decrease in a factor's price when its share in income is large, this will push the stratum's total income towards a decline. The earnings shares, $\alpha_{r,s,i}$, are obtained from GLSS 7 HH survey data while changes in factor returns/prices, $W_{r,s,i}$, are the outcomes of the general equilibrium model (along with the change in cost of living at the poverty line, C_r,).

2.3.3 Estimation of changes in the poverty headcount

Based on the projected changes in real income, changes in the poverty headcount in each stratum can be estimated using an elasticity of poverty. We instead use a HH microsimulation approach for greater precision. Using HH data for Ghana from GLSS 7 (Ghana Statistical Service, 2017), we shock the income of each individual HH in the neighborhood of poverty in the dataset, by the size of the change in real income caused by heat stress (as estimated using the approach described above). We then estimate poverty impacts by simply counting the portion of HHs whose incomes are pushed below the poverty line. Only HHs in the neighborhood of the poverty line are shocked, since these are the HHs that will move in and out of poverty. Assessing the impact of climate change on HHs across the full income range is beyond the scope of this study.

3 Results

3.1 Heat stress intensification

The projections show that both annual mean and maximum WBGT in West Africa will increase with global warming (Figure 3). Coastal regions will experience more serious mean-level heat stress than inland areas. Under global warming of 3.5°C or higher, annual mean WBGT is expected to reach 27 to 29°C across most of Ghana. This corresponds to the WBGT reference values for low and moderate metabolic rate in the ISO standard (see Annex 2, Table 6), meaning that labor capacity losses occur at this level of heat stress even for low intensity work, if heat injury is to be avoided. The inland regions are likely to experience the greatest rise in maximum WBGT (hence heat stress) due to the relatively large climate variability. These regions, including the northern part of Ghana, are expected to have annual maximum WBGT exceeding 39°C under a mean global warming scenario of 3.5°C.

Figure 3: Heat stress intensification in Ghana and parts of West Africa

A. Annual mean WBGT in baseline period (1961-1990) and under 1°C-4°C mean global warming

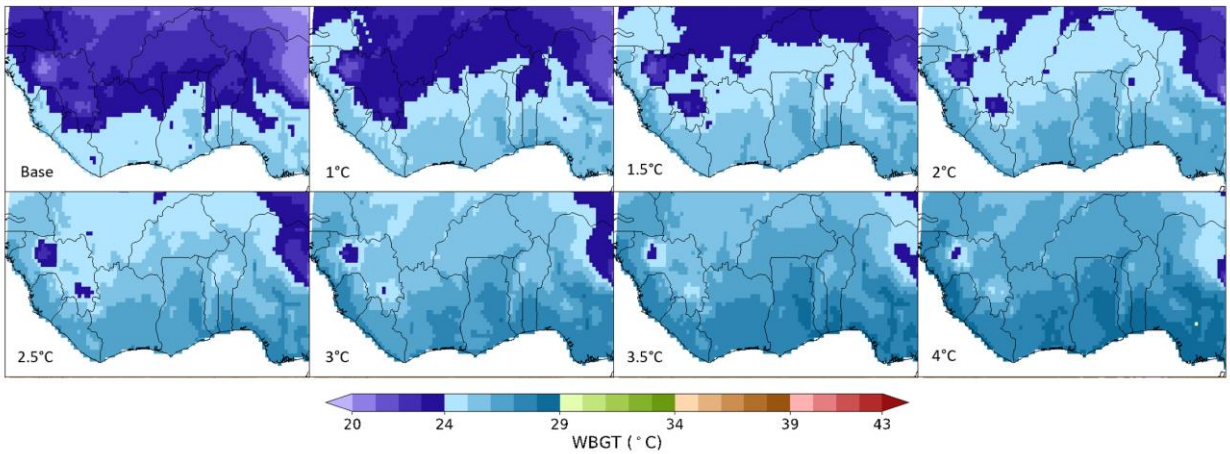

B. Maximum WBGT in baseline period (1961-1990) and under 1°C-4°C mean global warming

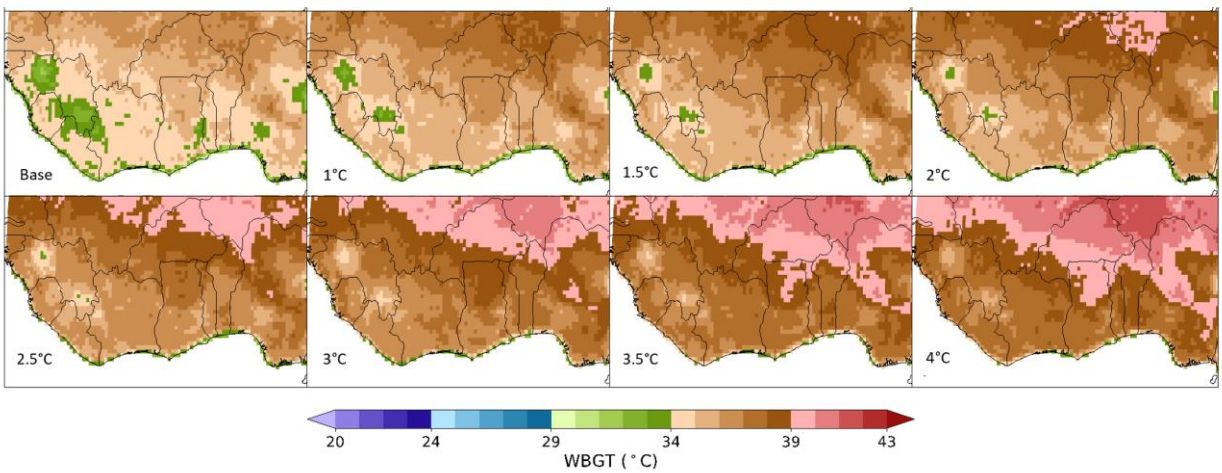

Furthermore, under 3°C warming, there will be more than one month each year that is hotter than the three hottest days in most of Ghana under the baseline situation. This number will exceed two months under 4 °C warming, particularly in coastal regions (Figure 4).

Figure 4: Number of days in each year that are hotter than the annual hottest 3 days during baseline period (1961-1990) under (a) 1.5 °C, (b) 2 °C, (c) 2.5 °C, (d) 3 °C, (e) 3.5 °C and (f) 4°C warming

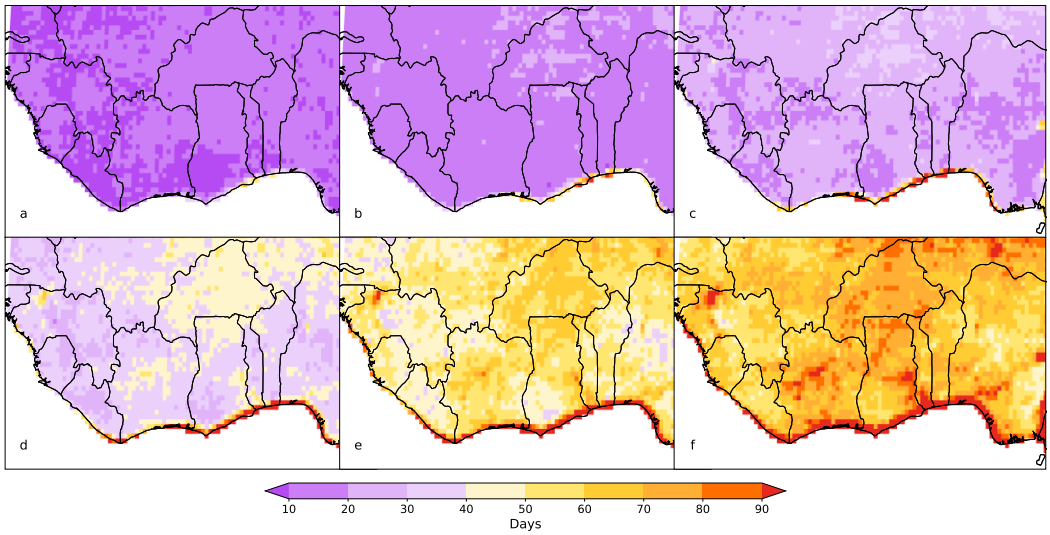

3.2 Labor Capacity Losses at the Grid Cell Level

As a result of the intense mean-level heat stress, Ghana will be seriously affected by reductions in annual labor capacity (Figure 5). Under a 3°C warming scenario, labor capacity is projected to drop below 65% for a metabolic rate of 400 W and below 55% for a metabolic rate of 600 W in most areas of the country. The situation becomes even more critical under 4°C warming, with labor capacity mostly less than 45% of the baseline value for a metabolic rate of 600 W. The central part of Ghana is most seriously affected.

Figure 5: Labor capacity loss in West Africa under different global warming scenarios and metabolic rates (days lost p.a.)

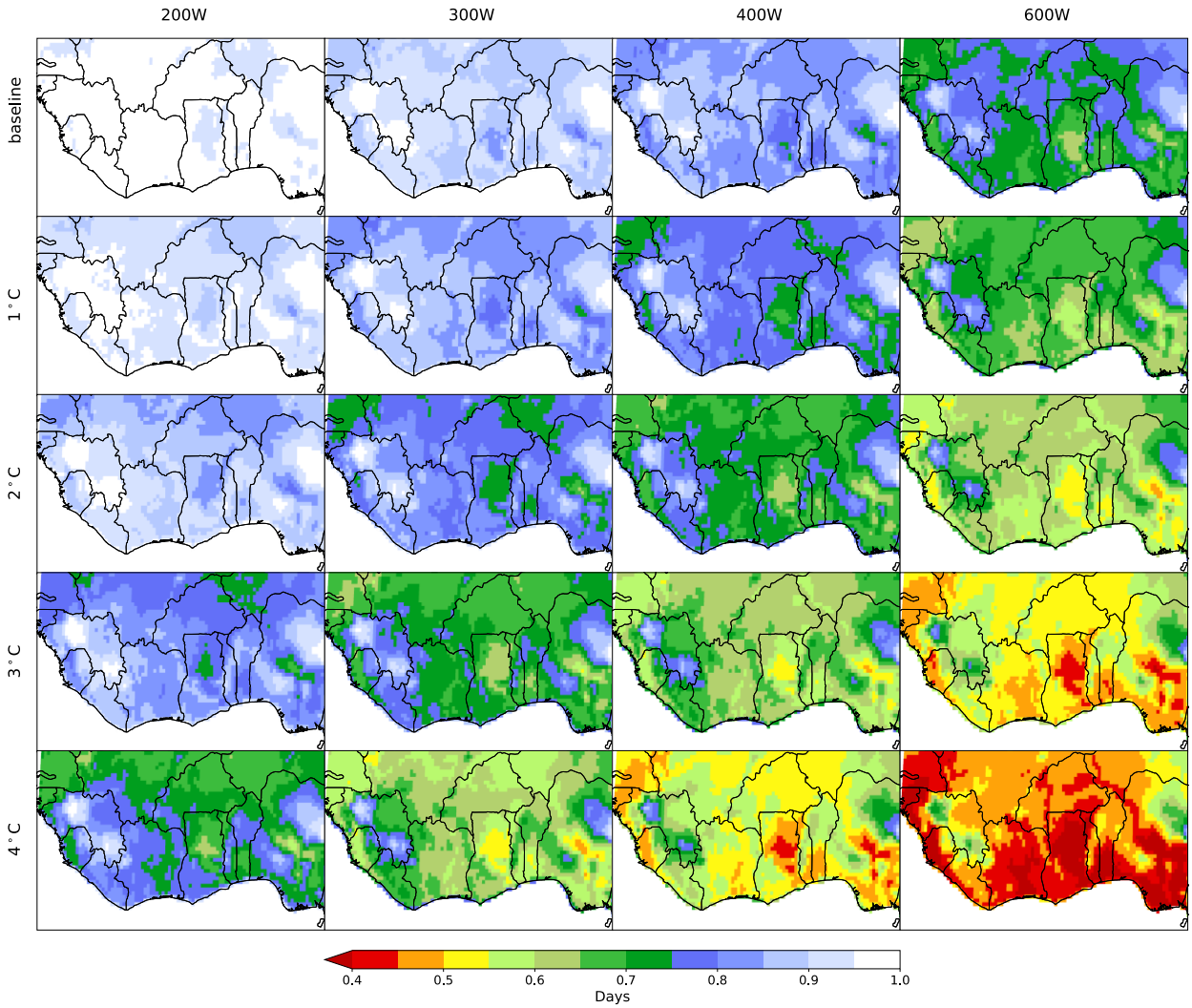

Notes: Constant outdoor working conditions are assumed. Only daytime hours are considered available for working.

Figure 6 presents the forecast reductions in the national average labor capacity of Ghana resulting from the different global warming projections. For a metabolic rate of 600 W, mean labor capacity will be around 50% of the baseline level under 3°C warming and is projected to approach 40% of the baseline under 4°C warming. The labor capacity reduction accelerates beyond 2.5°C warming.

Figure 6: National average labor capacity loss in Ghana under different warming targets and metabolic rates

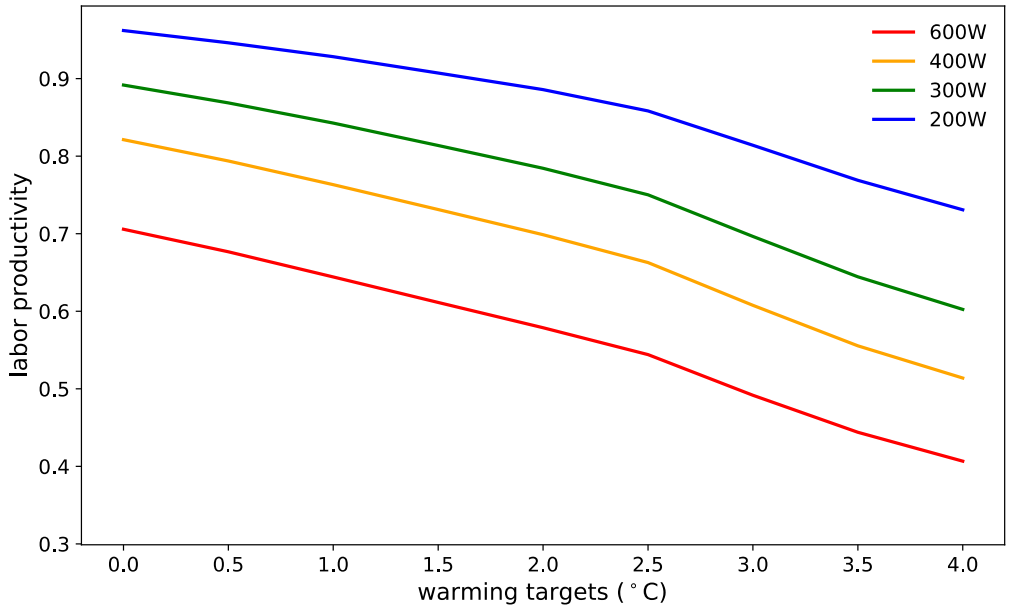

Notes: This figure assumes constant outdoor working conditions and daytime hours only available for working. Shaded area denotes the spread between maximum and minimum labor capacity across 14 Global Climate Model members.

3.3 Labor Capacity Losses by Sector and Labor Type

As detailed in the methodology section, estimated labor capacity losses according to work intensity (as shown in Figure 6) and work conditions (both outdoor and indoor) are translated into labor capacity losses by sector and by labor type (Figure 7). Only agriculture, manufacturing, and services are shown. The projections indicate, for example, that unskilled workers engaged in agriculture (bottom-right corner panel), if located in northern grid cells, will see labor capacity declines of 18% or more. These same workers, if located in more southern grid cells, will experience lower labor capacity losses of 14 to 16%. Labor capacity losses for unskilled workers in services (top-right corner panel) range between 10 and 16% in the northern half of the country, and between 6 and 8% in the southern half. Unskilled workers in manufacturing (middle-right panel) see smaller labor capacity losses than their counterparts in agriculture and services.

Figure 7: Labor capacity losses in Ghana under 3°C mean global warming, by sector and worker type

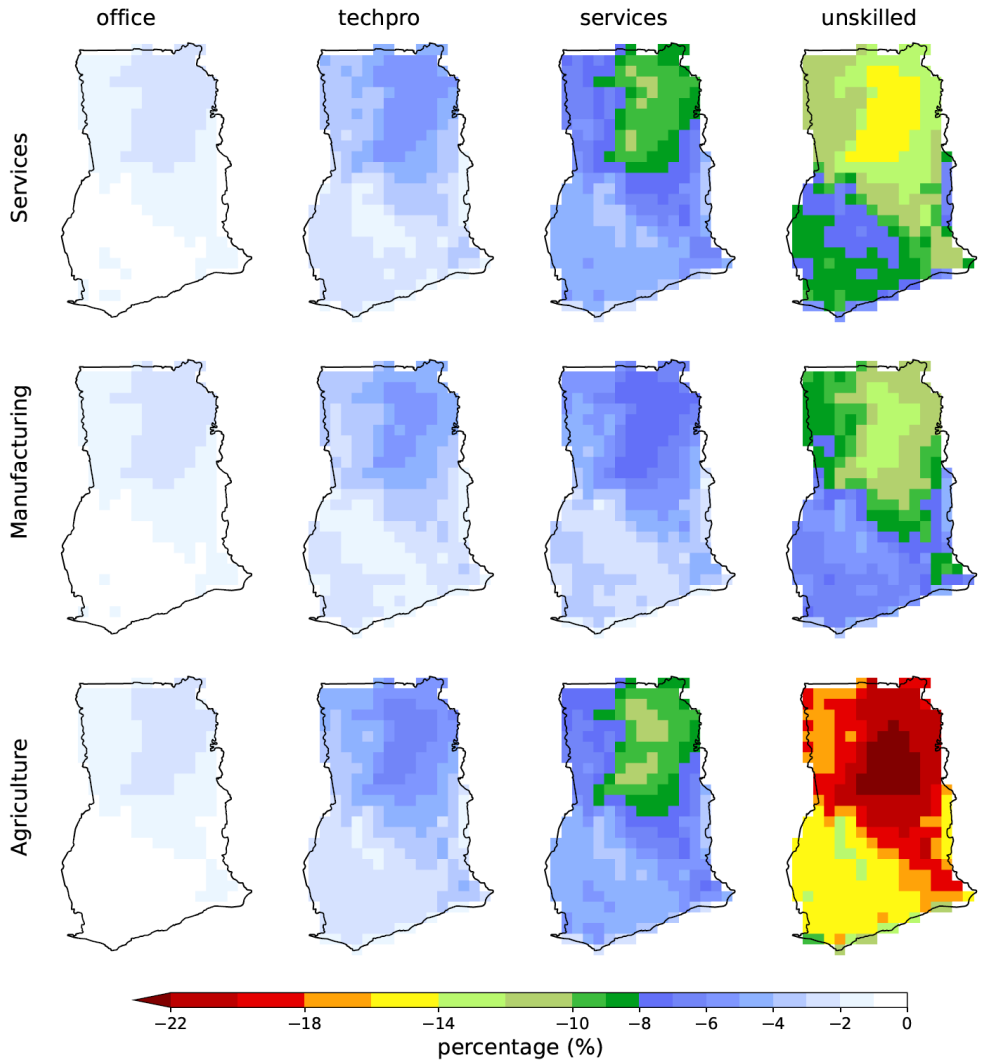

3.4 Country-Level Labor Capacity Losses

At the country level, we find that Ghana loses, on average, 6.4% of its labor capacity due to heat stress (Figure 8). This aggregated estimate accounts for the relative importance of different economic sectors as employers of labor, the types of workers these sectors employ, the varying intensities of work they perform, and the degree of outdoor exposure they experience. Based on this aggregate metric, out of 137 GTAP countries/regions, Ghana experiences the 16th largest labor capacity losses.

Figure 8: Country-level mean labor capacity losses under 3°C mean global warming scenario

A. Mean labor capacity losses across Africa (%)

B. Top 30 GTAP regions based on mean labor capacity losses (%)

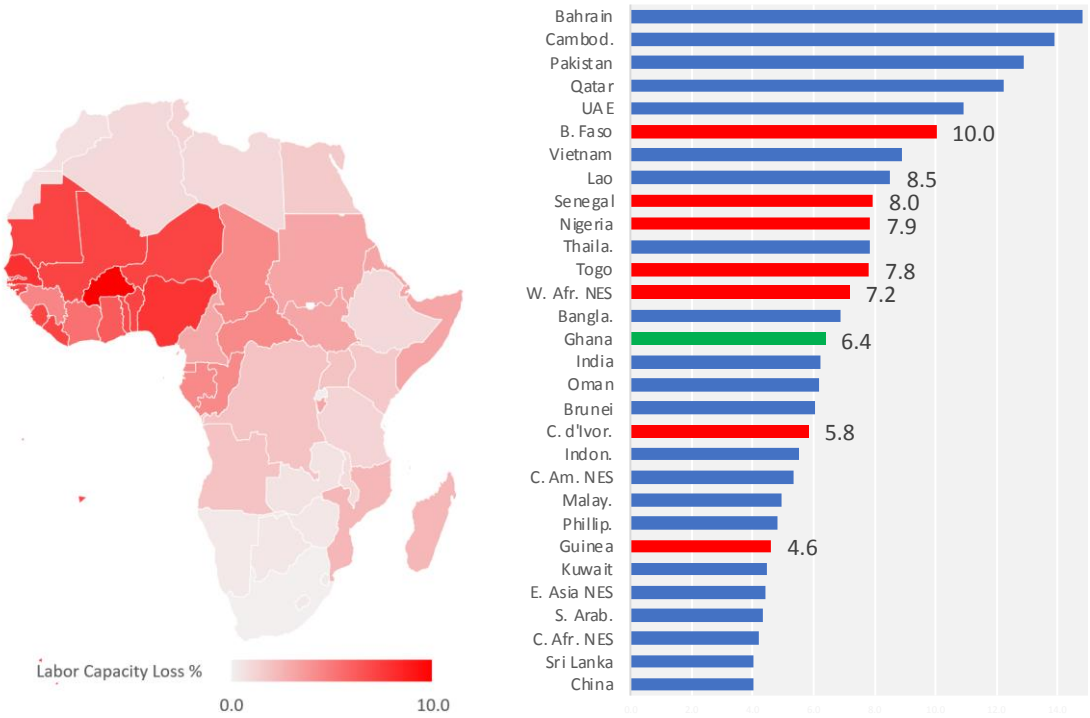

Notes: (1) W. Afr. NES includes Benin, Cape Verde, the Gambia, Guinea-Bissau, Liberia, Mali, Mauritania, Niger, Saint Helena and Sierra Leone; (2) E. Asia NES includes Democratic People's Republic of Korea and Macao Special Administrative Region of China; (3) C. Am. NES includes Belize; (4) C. Afr. NES includes Central African Republic, Chad, Congo, Equatorial Guinea, Gabon, and Sao Tome and Principe.

Our estimates are subject to uncertainty as they depend on the climate model used. Out of the 14 Global Climate Models (ensemble members) sampled, the majority place Ghana's aggregated labor capacity loss between 5.9 and 6.7% (Figure 9).

Figure 9: Labor capacity losses in Ghana for different climate model ensemble members under 3°C mean global warming

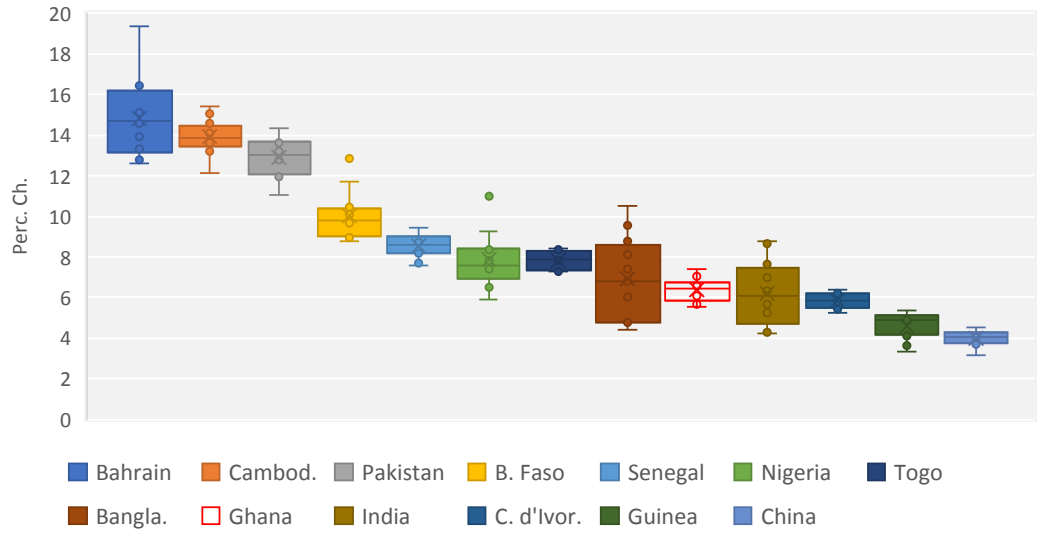

Notes: Boxes show the interquartile range of labor capacity losses from 14 different climate model ensemble members. Horizontal lines indicate the 75th, 50th and 25th quartiles. Means are indicated with an x. Whiskers/error bars indicate the range from maximum to minimum.

3.5 Sector-Level Labor Capacity Losses

While Ghana loses 6.4% of its labor capacity, on average, at country level, sectoral disaggregation shows that agriculture is disproportionately impacted and loses 16% of its labor capacity. This is important in a country where agriculture employs over a quarter of all labor (see Panel A of Figure 10).

Within sectors, as we might expect, 'blue-collar' workers are more impacted than other worker types as they tend to perform the highest intensity labor and work outdoors more frequently. Panel B of Figure 10 shows the extent of the disparity: blue-collar workers lose at least twice as much of their work capacity as other workers in the same sectors. The figure also shows that the hardest-hit subgroups are, in order, blue-collar workers in agriculture, construction, and mining. These workers lose more than 12 to 16% of their labor capacity. Furthermore, it is in agriculture that blue-collar workers account for over 90% of the sector's labor value-added in the base.

Figure 10: Labor capacity losses in Ghana, by sector and worker type, under 3°C mean global warming

A. Labor capacity loss by sector

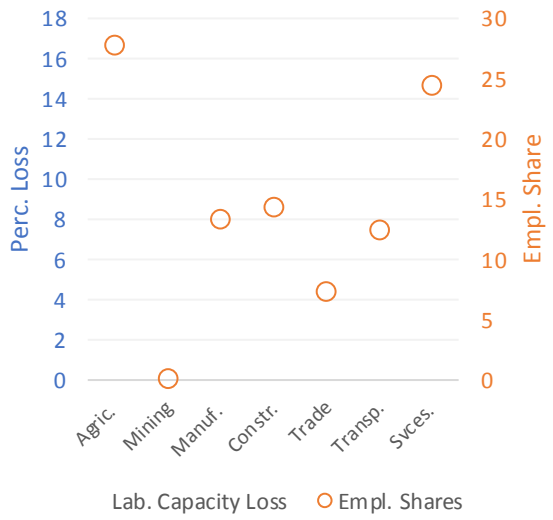

B. Labor capacity loss by sector and worker type

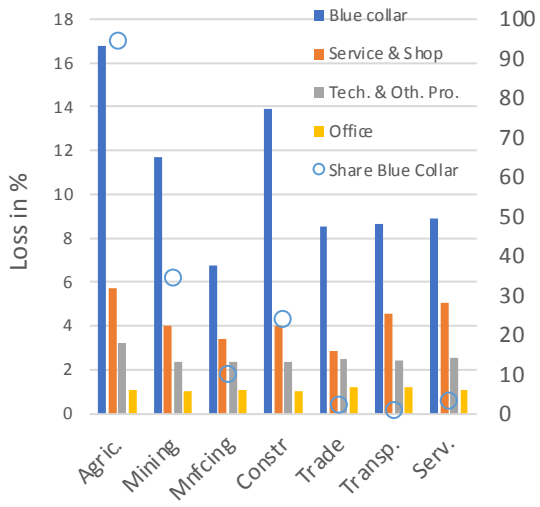

Notes: Bars indicate results under 3°C mean global warming.

3.6 Changes in Value-Added by Sector

Labor capacity losses in turn lead to losses of output and value-added. Figure 11 shows the relative magnitude of loss of real value-added across 65 disaggregated sub-sectors. These losses contribute, in turn, to losses in real GDP in the Ghanaian economy (see below). We find that the largest relative loss of value-added occurs in the 'other crops' and the 'vegetable and fruits' sectors, followed by the construction sector. This is reflective of these sectors' dependence on blue-collar workers, who are expected to experience large labor capacity losses due to a combination of high-intensity activity and exposure to solar radiation through outdoor work. The relatively large size of these sectors' value-added in the base (see Annex 2, Figure 23) also plays an important role in this outcome.

Figure 11: Change in real value-added by sector under 3°C mean global warming

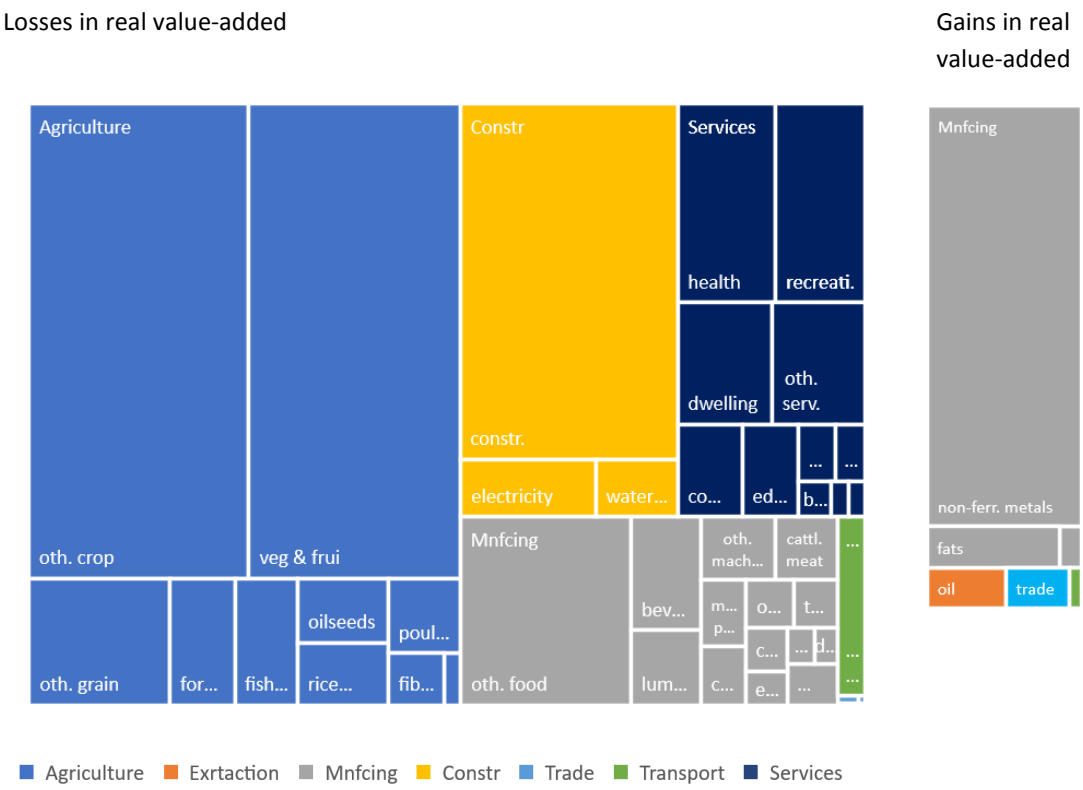

A small number of sectors also see their value-added increase (Figure 11, Panel B). In the case of non-ferrous metal products (which includes gold), this increase is substantial and is larger than the decrease in value-added in all other manufacturing sub-sectors combined. This increase in value-added for non-ferrous metals is linked to export demand. This can be seen in Figure 12, which presents changes in each sector's domestic and export demand. For non-ferrous metals, there is a large percentage increase in export demand, and since gold is among Ghana's top exports, this translates to a large increase in value-added. In contrast, the wool sector also sees a large percentage increase, but this sector and its exports are small in the base.

Figure 12: Percentage changes in domestic and export demand by sector under 3°C mean global warming

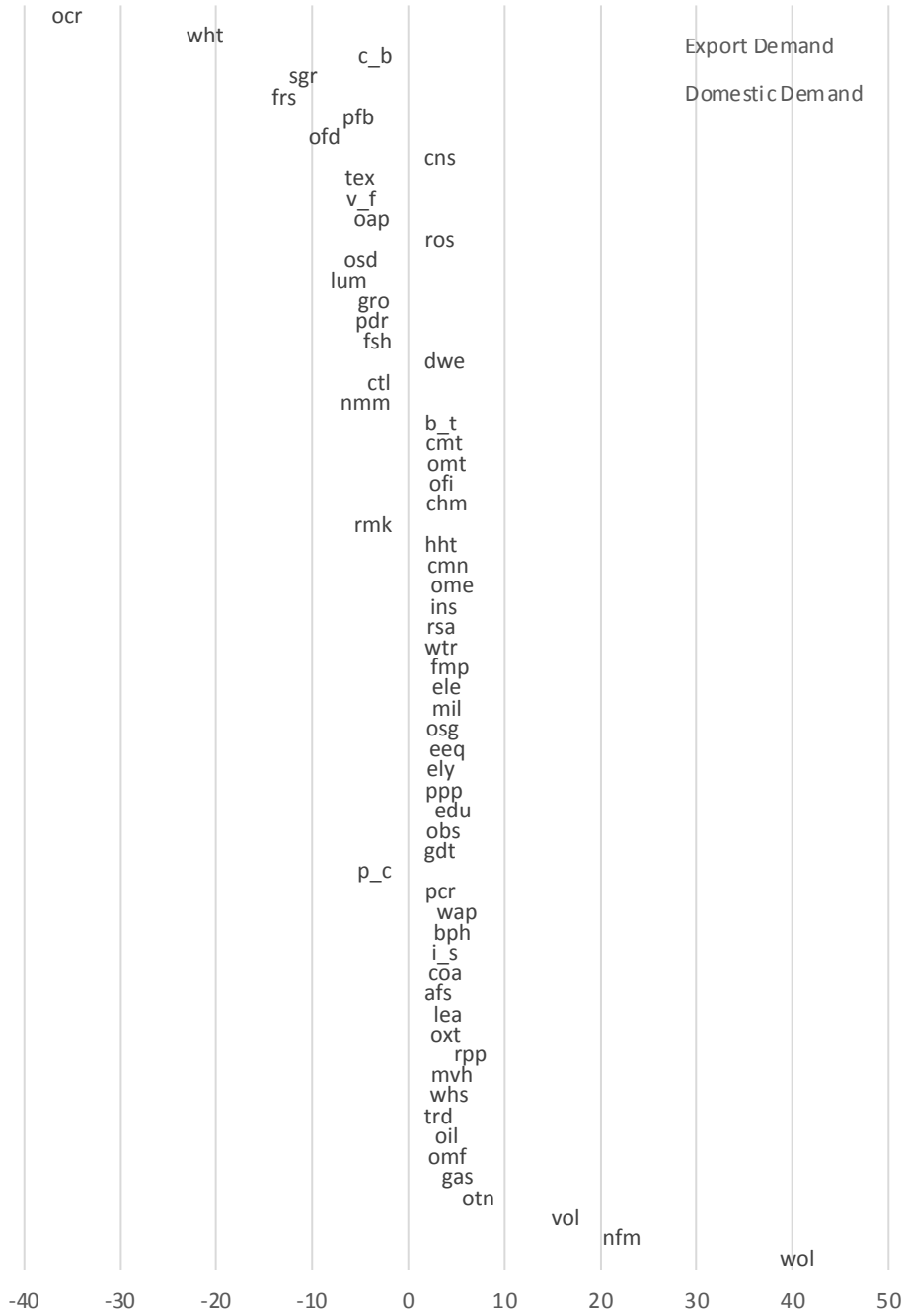

3.7 Agricultural Output and Prices

Figure 13 provides a more detailed view of the agricultural sector, since output and price changes in in agriculture have a direct bearing on food security. As already indicated in Figure 11, 'fruits and vegetables' and 'other crops' are important in Ghana and both suffer large losses in value-added. From Figure 13, we see the output of most food crops decline by 5% or more. The exception is 'Other Crops' (OthCrop), which see a 24% decline, explained by a sharp reduction in export demand (as shown

previously in Figure 12). The same is true for livestock sectors ('cattle' and 'OthLvstk'). As would be expected, falls in output cause prices to rise. For most food crops, prices rise by 9 to 12%.

Figure 13: Changes in output and prices of agricultural sectors under 3°C mean global warming

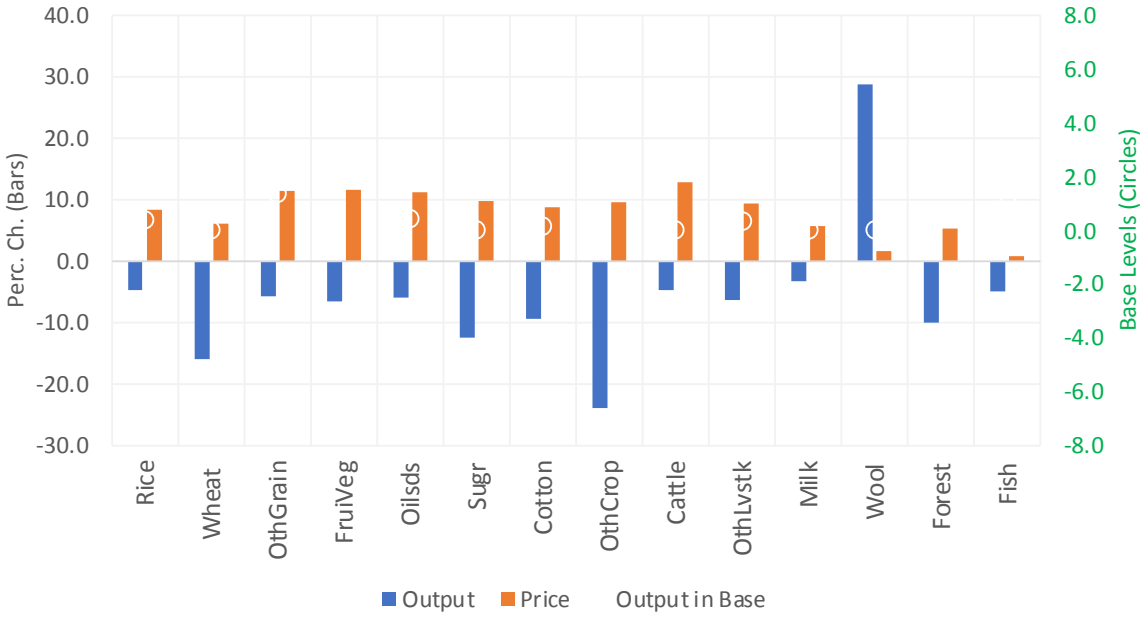

3.8 Employment

Our results indicate a movement of blue-collar labor into agriculture from other sectors, most notably from construction (Figure 14). Employment of blue-collar workers in construction falls by more than 6% and increases in agriculture by 1%. (Recall from Figure 10 that agriculture has a much larger share of blue-collar employment in the base.) Furthermore, the construction sector sees declines of all other types of workers as well as capital.

These employment outcomes are the result of two, potentially opposing, mechanisms on the supply side. Loss of productivity of labor, on the one hand, increases demand for labor in every sector. This is because as a unit of labor becomes less productive, more labor is needed to prevent output losses. However, competition for labor across sectors, substitutability of labor with capital across different sectors, as well as the mobility of labor between sectors determines which sectors are able to draw in labor and which sectors contract in size and cede labor to other sectors.[5]

In this experiment, blue-collar labor is pulled into agriculture due to the second mechanism, in order to dampen output losses and moderate the strong price increases resulting from the price-inelastic nature of food demand. In the case of construction, facing a more price-elastic demand, the sector

[5] In our application of the GTAP-POV model, labor is assumed to be imperfectly mobile between agricultural and non-agricultural sectors. Furthermore, we assume fixed aggregate employment of labor in the economy.

contracts and loses resources to other sectors. The services sector also follows a similar pattern as construction. Manufacturing, which includes non-ferrous metals, sees a large increase in export demand (as climate change is a global shock, affecting production elsewhere too), therefore contributing to increased employment of labor as well as capital.

Figure 14: Employment of labor and capital by aggregate sector under 3°C mean global warming

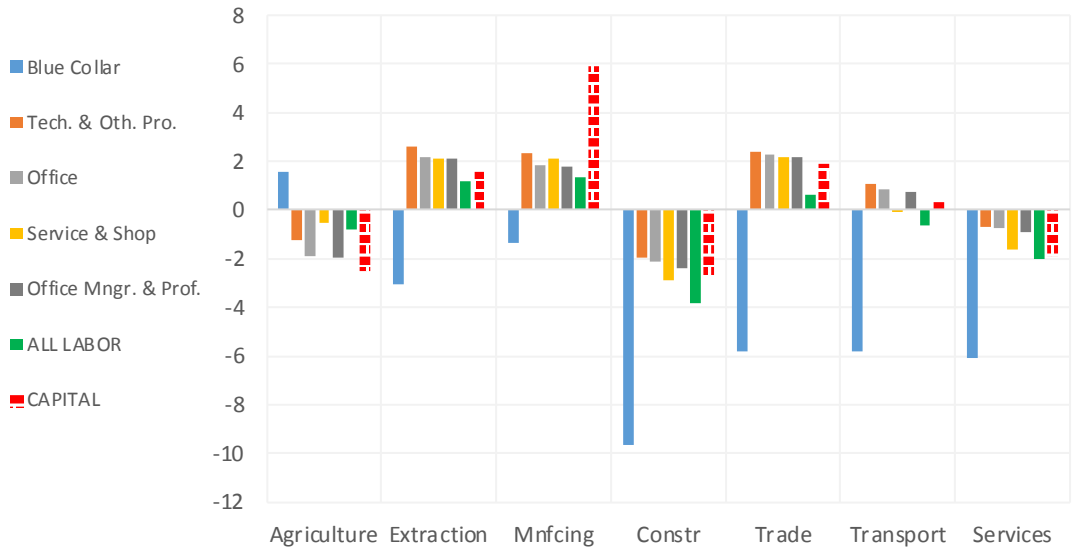

3.9 Real GDP and Terms of Trade

Ghana is projected to experience a sharp decline in its overall GDP. This decline is particularly striking, when compared to its aggregated labor capacity loss; despite having the 16th largest labor capacity loss (Figure 8), Ghana has the 4th largest GDP loss (Figure 15, Panel A). This reflects the composition of labor capacity losses, which interacts with the structure of the Ghanaian economy. When labor productivity declines disproportionately in agriculture, one adaptive response for the economy is to draw in labor from other sectors less affected by heat stress, in order to dampen output losses. However, for economies that already employ a large portion of labor in agriculture, this response is constrained, hence output declines sharply.

However, it should also be noted that Ghana's GDP results show significant uncertainty (Figure 15, Panel B). In particular, there is a larger spread of predicted values than for other countries with large GDP declines. Nonetheless, the majority of climate models result in Ghana's GDP falling by 3.3 to 5.4%. Even after considering model uncertainty, Ghana still experiences one the largest GDP declines out of the 137 GTAP regions.

Figure 15: Impacts on GDP under 3°C mean global warming

A. Top 30 GTAP regions with largest GDP loss (%)

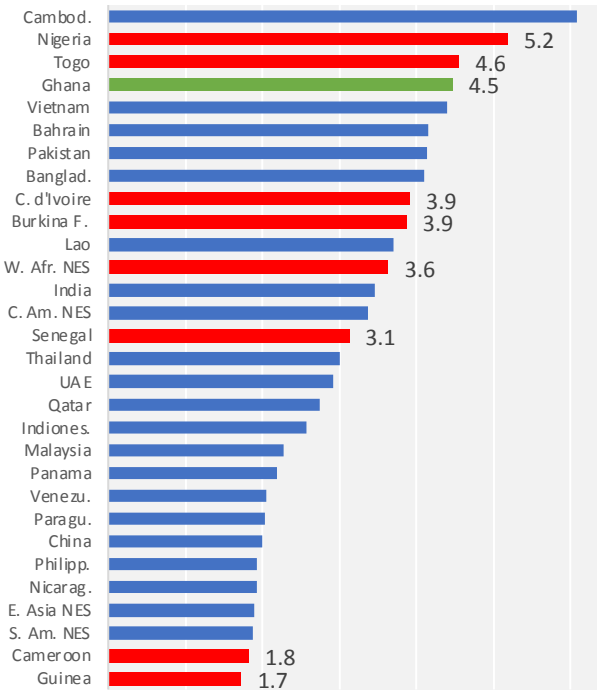

B. Range of GDP Changes in Ghana and selected countries

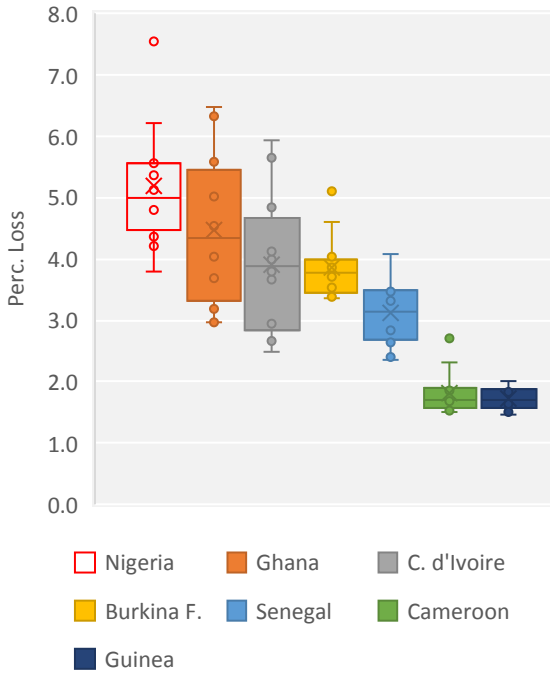

Notes: Boxes show the interquartile range of labor capacity losses from 14 different climate ensemble members. Horizontal lines indicate the 75th, 50th and 25th quartiles. Means are indicated with an x. Whiskers/error bars indicate the range from maximum to minimum.

Ghana does however, on average, experience a slight improvement of 0.7% in its terms of trade of (Figure 16). This is an indication of its ability to share some of the cost of its relatively severe climate change impacts with countries importing Ghana's products. Formally, a country's terms of trade are a measure of a country's export prices relative to its import prices. In this case, the prices of goods that Ghana exports improve relative to prices of goods that it imports.

Figure 16: Percentage changes in Terms of Trade in Africa under 3°C mean global warming

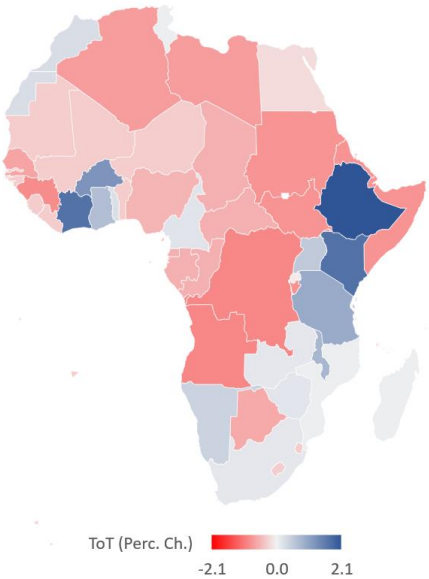

3.10 Impact on the Poor

As described in the methods section, we determine changes in the poverty headcount that result from heat stress-induced labor capacity losses using a two-step, macro-to-micro approach. In the first step, we determine how much incomes are affected for HHs near the poverty line, given changes in prices and factor returns determined in the main macro model. In doing so, we account for the fact that HHs vary in how they earn their income. Recall from section 2.3.2 that the income of stratum s in region r is determined by:

$$Y_{r,s} = \sum_i \alpha_{r,s,i} \left(W_{r,s,i} - C_r\right)$$

Our results indicate that, for HHs in the neighborhood of absolute poverty (income of $1.90/person/day), considering the spending patterns of these HHs, the real cost of living in Ghana (C in the equation above) increases by about 3.2%. This increase is driven largely by the 11% increase in the price of crop commodities (as a composite), which account for an estimated 20% of poor HHs' spending. Thus, nearly three quarters (73%) of the increase in the cost of living for poor HHs can be attributed to price increases of crops (Table 1). This is followed by other food products (+19% of the overall increase in the cost of living at the poverty line).

Table 1: Contribution of different commodity groups to the increased cost of living for households at the international poverty line under 3°C mean global warming

Commodity Group	Share in budget of poor HHs (%)	Change in Composite Price (%)	Relative contribution to increase in cost of living (%)
Crops	20.8	11.2	72.5
Other Food	19.6	3.0	18.5
Manufacturing	38	0.4	5.3
Apparel	12.4	0.9	3.4
Meat & Dairy	1.2	1.5	0.6
Utilities	4.7	0.1	0.1
Trade	0	0.5	0.0
Transport & Communication	0.9	0.1	0.0
Financial services	0	-0.8	0.0
Other services	2.4	-0.5	-0.4
Total	**100.0**		**100.0**

As for nominal income, this is determined by factor prices ($W_{r,s,i}$), while considering the fact that HHs in the neighborhood of the poverty line vary in terms of how they earn their income, and thus which factor prices are important. This is captured by the earnings shares, $\alpha_{s,j}$, in the equation above (see section 2.3.2 for greater elaboration of the determination of earnings shares and incomes). As noted above, these changes in nominal income are adjusted for the cost of living, to obtain changes in income in real terms.

Table 2 shows the resulting mean estimate of changes in real income. We see that non-agricultural HHs at the poverty line see the largest mean decline in real income (5.9%), while agricultural HHs that rely on unskilled labor to a large extent see the smallest decline (0.5%). The interquartile ranges around the changes in real income are illustrated in Figure 17, which shows that the majority of results lie approximately within 2 percentage points of the mean result.

Table 2: Percentage changes in real income of households at the poverty line, by strata

Strata	Percentage change in real income
AGRICULT	-0.5
NNAGRCLT	-5.9
URBLABOR	-5.0
RURLABOR	-2.6
TRANSFER	-5.3
URBDIVRS	-3.6
RURDIVRS	-2.4

Notes: HH strata are defined as follows. **AGRICULT**: HHs that earn more than 95% of their income from agricultural self-employment; **NNAGRICULT**: HHs that earn 95% of their income from non-agricultural self-employment; **URBLABOR**: urban HHs that earn 95% of their

income from wage labor; **RURLABOR**: rural HHs that earn 95% of their income from wage labor; **TRANSFER**: HHs that earn 95% of their income from transfers; **URBDIVRS** and **RURDIVRS**: urban and rural HHs that do not fall under any other category.

Figure 17: Percentage change in real incomes by strata under different ensemble members under 3°C mean global warming

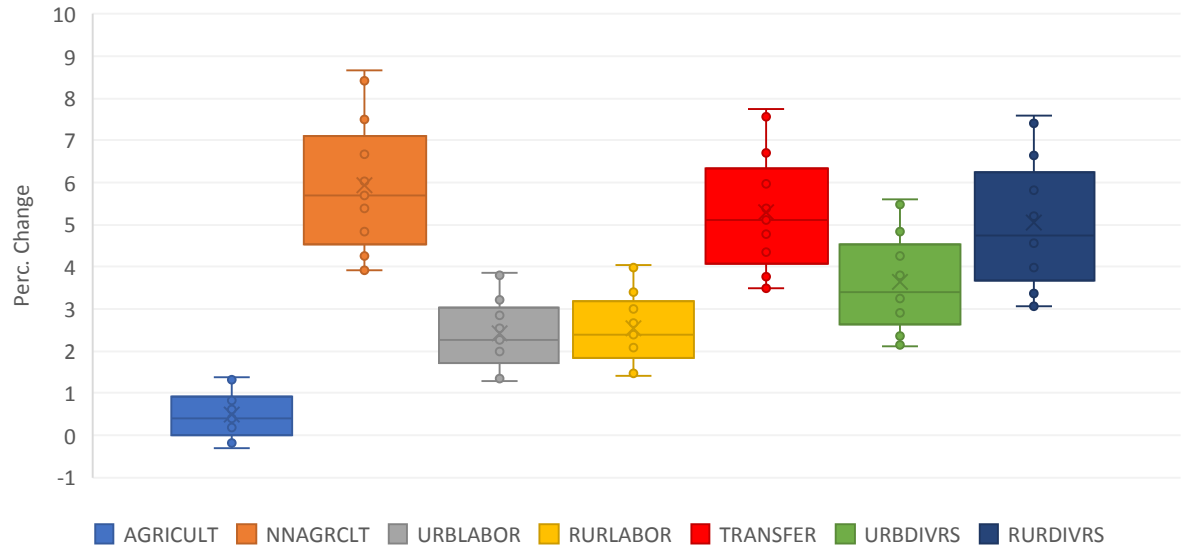

Notes: Boxes show the interquartile range of real income losses from 14 different climate ensemble members. Horizontal lines indicate the 75th, 50th and 25th quartiles. Means are indicated with an x. Whiskers/error bars indicate the range from maximum to minimum.

In step 2, we implement a HH microsimulation using these incomes changes. Using HH income survey data for Ghana from GLSS 7, we shock the real income of individual HHs that lie within a decile around the poverty line, by the size of the income declines reported in Table 2. The (weighted) numbers of HHs that fall within this decile by strata are reported in Table 3. We then count the number of HHs that fall in (or out) of poverty as a result of the income change.

Table 3: Distribution of households within one decile of the poverty line

Stratum	**No. of HHs within 1 decile of poverty line**		**Total**
	No	**Yes**	
Agriculture	4,866,658	540,329	5,406,987
	19.8%	21.0%	19.9%
Non-Agriculture	4,652,373	363,173	5,015,546
	19.0%	14.1%	18.5%
Urban Labor	2,246,916	248,778	2,495,694
	9.2%	9.7%	9.2%
Rural Labor	584,843	65,051	649,894
	2.4%	2.5%	2.4%
Transfer	550,342	60,782	611,124
	2.2%	2.4%	2.3%
Urban Diverse	5,301,037	589,259	5,890,296
	21.6%	22.9%	21.7%

Rural Diverse	6,354,314	705,671	7,059,985
	25.9%	27.4%	26.0%
Total	**24,556,483**	**2,573,043**	**27,129,526**
	100.0%	**100.0%**	**100.0%**

Notes: The poverty line for Ghana in local currency terms is set to be consistent with a 12.7% poverty rate as reported by the World Bank WDI for Ghana in 2017, using the $1.90 per day international poverty line.

Figure 18 below shows the estimated mean percentage change in poverty using this approach. Overall, Ghana sees a 2.2% increase in poverty. Given a poverty headcount in the base year (2017) of around 3.5 million, a 2.2% increase represents approximately 76,000 additional people falling into poverty. The figure shows that a large portion of the increase in poverty is driven by the rural diverse ('RURDIVRS') stratum, followed by the transfer ('TRANSFER') and urban diverse ('URBDIVRS') strata. The RURDIVRS stratum refers to rural HHs that are not specialized, i.e., they earn less than 95% of their income from any single source (wage labor, self-employment or transfer payments). The rural diverse stratum sees a 3.9% increase in poverty and has the second largest population of poor people in the baseline. The first largest population of poor lies in the agricultural stratum. This stratum sees little change in poverty, however. This is explained by the large share of unskilled labor in the earnings of agricultural HHs,[6] and the fact that unskilled labor experiences an increase in its returns. This is described further below.

Figure 18: Impacts on poverty by strata under 3°C mean global warming

A. Percentage changes in poverty

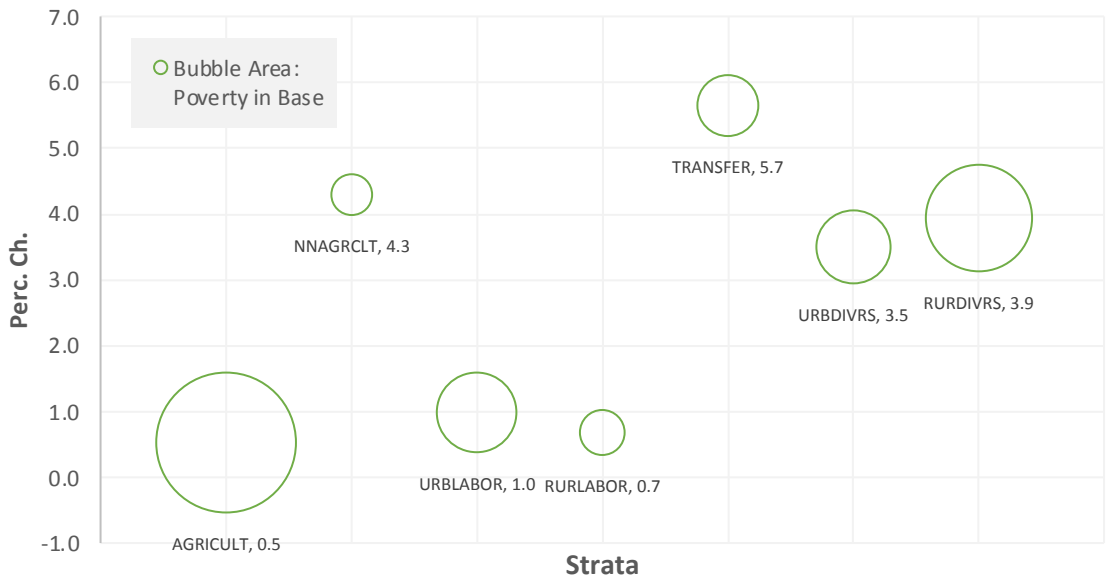

[6] Recall from the methods section that the share of unskilled labor relative to skilled labor for the agricultural stratum was adjusted to be consistent with skilled-unskilled portions in the GTAP database, which are in turn obtained from ILO data.

B. Changes in poverty in numbers

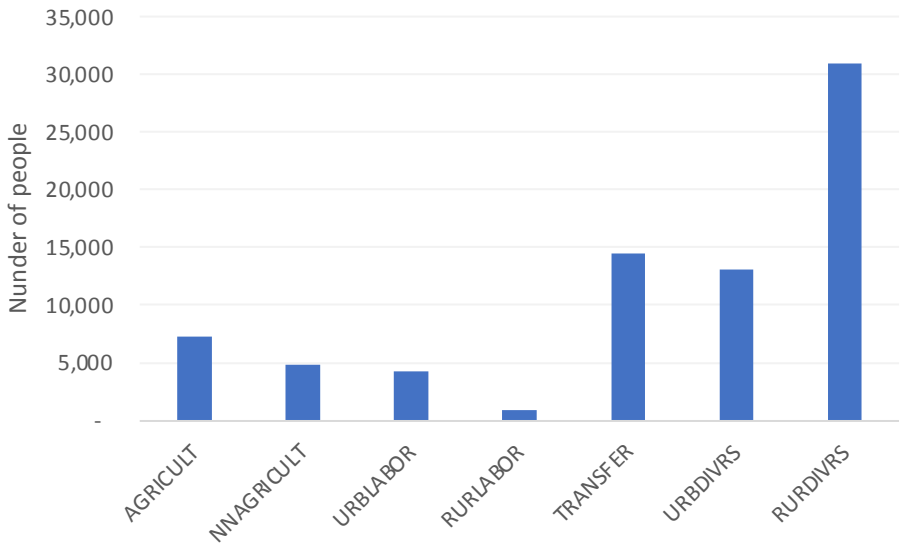

Figure 19 illustrates the uncertainty around these poverty outcomes by showing the interquartile range of the estimated poverty impacts using the different estimates of labor capacity losses generated by the 14 different climate models. It shows that for most strata, while there are outlier results, the range of the majority of results is narrow.

Figure 19: Percentage change in poverty in Ghana under different ensemble models under 3°C mean global warming

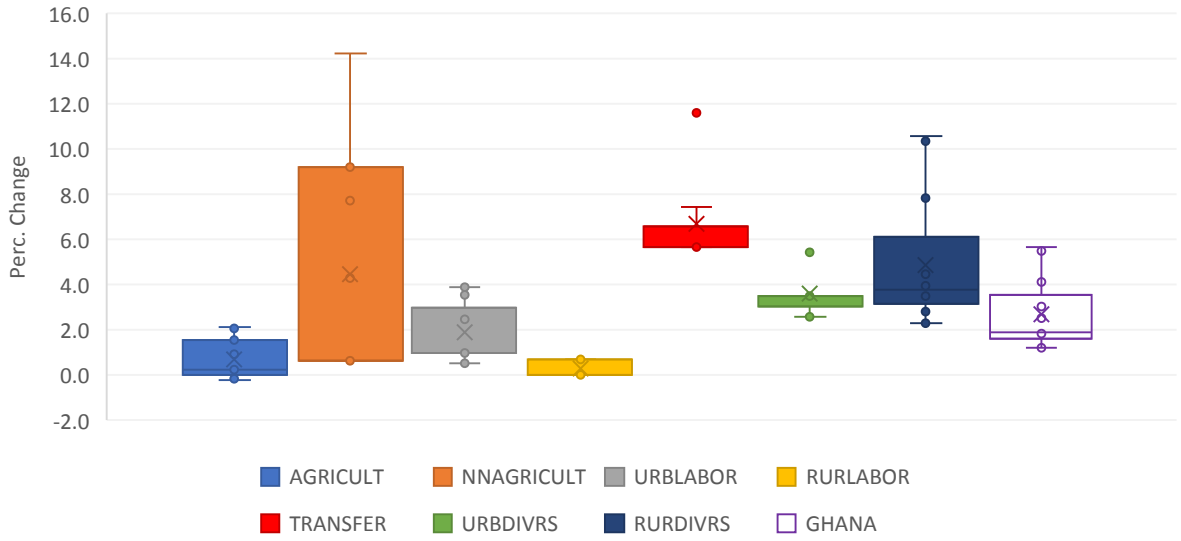

Notes: Boxes show the interquartile range of percentage change in poverty from 14 different climate ensemble members. Horizontal lines indicate the 75th, 50th and 25th quartiles. Means are indicated with an x. Whiskers/error bars indicate the range from maximum to minimum.

The size of the percentage change in poverty for any particular stratum is explained by two things: (i) the size of the stratum's income shock (which in turn depends on changes in returns to different

factors and the importance of these in the total income of the stratum), and (ii) the density and distribution of HHs that lie just above the poverty line within each stratum

Figure 20 shows that unskilled agricultural labor is the only factor that experiences an increase in returns, relative to the cost of living at the poverty line. This is because of the strong decline in the productivity of unskilled labor due to heat stress. This decline effectively creates a shortage of this type of labor, causing its price/wages to increase. The real returns paid to all other factors decline however, due to the diminished productivity of labor.

Figure 20: Change in real incomes of factors of production at the poverty line under 3°C mean global warming

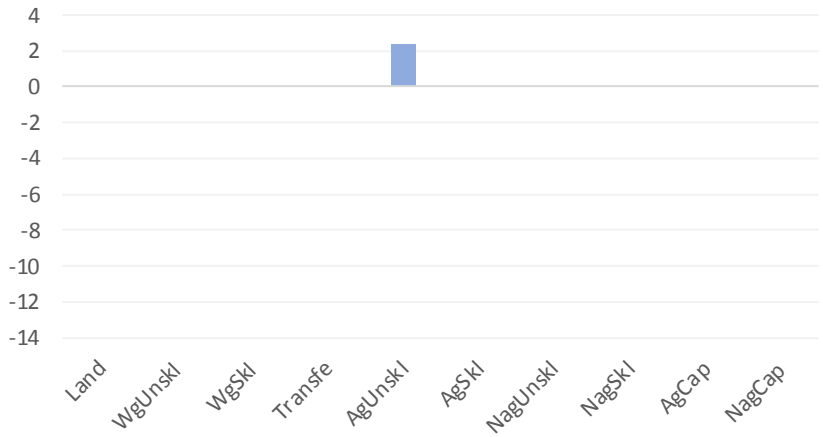

Figure 21 shows the earnings shares of each stratum (this is the same as Figure 2 from the methods section). We can now see why the agricultural stratum sees little change in poverty: real returns to agricultural unskilled labor are increasing and its earnings share in the agricultural stratum's income is large.

Figure 21: Earnings shares at the poverty line, by strata

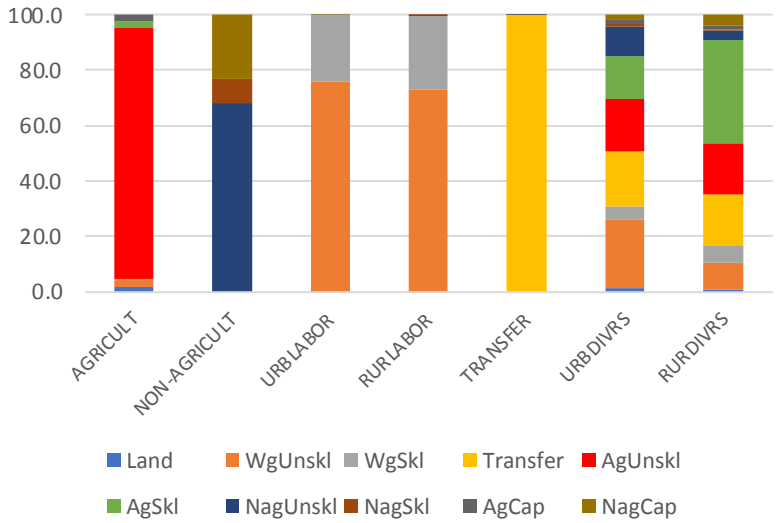

Finally, Figure 22 illustrates the distribution of HHs around the poverty line for the urban labor stratum (which sees a small increase in poverty) and the rural diverse stratum (which sees the largest increase in poverty). The figure also shows the shift in this distribution caused when real incomes of HHs within one decile of the poverty line decline by the amounts shown previously in Table 2. Note that these two strata have similar declines in income (in Table 2), but for the rural diverse stratum, there is simply a larger number of HHs just above the poverty line who are impacted and pushed into poverty.

Figure 22: Change in income distribution at the poverty line before (green) and after (red) heat-stress induced decline in real income in selected household strata

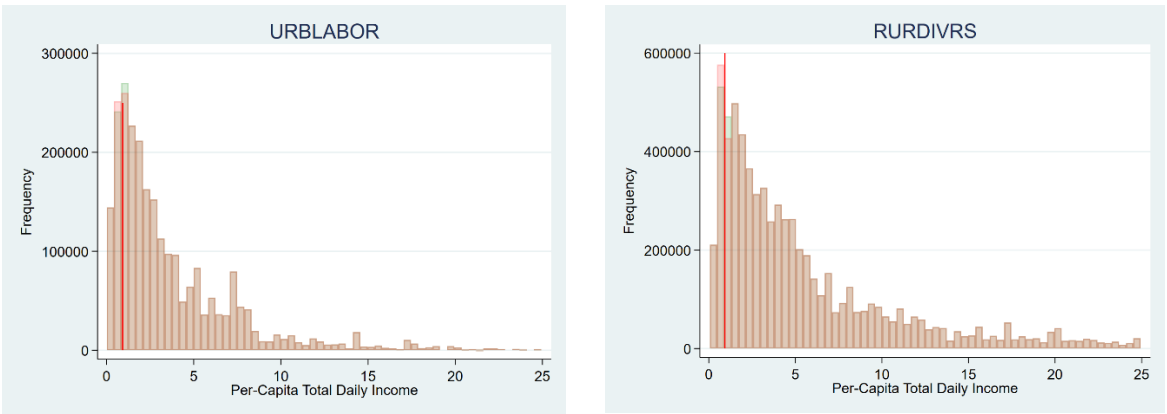

Notes: Red vertical line shows the poverty line in national currency terms. Each figure shows two sets of bars overlaid. Green bars show distribution of poverty before heat stress induced decline in real income; red bars show distribution after decline in real income. The income shock is only administered to HHs in each strata that lie within 10% of the poverty line. Incomes of all other HHs are held constant. Thus, changes in severity of poverty and inequality is not adequately captured in this approach.

4 Discussion and Policy Responses

Most studies of climate impacts on agriculture and food prices have ignored human heat stress, focusing instead on the consequences for crops. Yet recent work suggests that the impacts of human heat stress on farm workers' productivity may be more significant in some of the poorest countries of the tropics (de Lima, et al., 2021). This report has focused on the way climate change affects human heat stress. But in this context, we have considered only the consequences for labor productivity. We have not explored the health impacts of heat stress and its associated costs (IPCC, 2014) (Patz, Frumkin, Holloway, Vimont, & Haines, 2014). We have also not considered the potential impacts on the disutility of manual, outdoor labor under these conditions (Hsiang, 2021). And beyond the impact of heat stress on humans, there are similar impacts on livestock (Mader, 2014) (Key & Sneeringer, 2014). However, given the many different species of livestock, a global assessment of these impacts is challenging.

By focusing on human heat stress and labor productivity across the entire economy, with a special emphasis on Ghana, the report has identified a number of important vulnerabilities. Due to their heavy reliance on outdoor manual labor, agriculture and construction are projected to be the most affected sectors of the economy. Since food is a necessity, the loss in productivity leads to a sharp price rise, thereby drawing additional labor into the sector to mitigate the decline in production. In the case of construction, the loss in productivity results in a significant output contraction and the sector sheds workers. Adaptation through increased mechanization moderates these adverse effects but is not sufficient to eliminate them.

The poverty impacts of climate-induced labor productivity losses are driven by two forces. Given the large budget share devoted to food by HHs at the poverty line, the sharp rise in food prices is an important driver of poverty increase. In addition, the productivity losses have significant impacts on factor returns, and hence HH income. Returns to farmland and capital fall as a result of the diminished productivity of unskilled farm workers. However, due to the climate-induced labor scarcity, the real earnings of unskilled farm workers rise enough to more than offset the impact of higher food prices. This does not mean, however, that they are better off, as we have not considered the health effects of the increased heat stress, as well as the disutility associated with farm work under these more stressful conditions.

It should also be borne in mind we have only reported changes in the poverty headcount. This provides only a partial view of the poverty impacts of heat stress-induced labor capacity losses, as this metric does not adequately describe increases in the intensity of poverty. Such changes are likely to be important but are beyond the scope of this study.

Other important limitations of this report relate to the estimations of earnings shares and the share of outdoor labor. Under the methodology applied, these are key parameters affecting poverty headcount results. For earnings shares, there is some uncertainty around the relative shares of skilled and unskilled labor, as Ghanian HH survey data and data from the ILO differ considerably. With regards to the share of outdoor labor, there is a lack of country-specific data. Ideally, we require data similar to that collected for the U.S. where the BLS reports indicators of the frequency of outdoor exposure of different labor types in different sectors. In the absence of such data, we are forced to estimate these shares for other countries by assuming that outdoor exposure and GDP per capita are logarithmically related.

This study could therefore be improved with better data. Furthermore, recent studies suggest that enhanced labor mobility can facilitate adaptation to climate change (Colmer, 2021). This is an avenue that deserves further exploration. The differential impact on labor across different skill types and sectors suggest that there will indeed be potential 'gains from trade' in more mobile labor as the economy seeks to adjust to these significant shocks.

Annex 1: Detailed methodology

The methodology applied and described in this annex is based on an on-going research study by Saeed et al. (Labor Heat Stress under a Warming Climate Increases Poverty across the Tropics, 2021).

Climate Data

In this study, we employ the outputs of 11 Global Climate Models (14 ensemble members) obtained from the CMIP6 archive for calculating WBGT (Table 4). Variables relevant for WBGT calculations are retrieved at 3-hourly frequency. The historical and Shared Socioeconomic Pathway (SSP) 585 experiments are used to quantify heat stress at a baseline period (1961-1990) and a 3°C warming world, respectively. To locate the period corresponding to a 3°C warming, we index each year in the SSP585 simulation by the degree of warming (compared with the baseline period) and select years falling into a range of 2.75 to 3.25°C warming, which are then used to represent a 3°C warming world.

Table 4: CMIP6 models used in this paper

Model	Ensemble member
ACCESS_CM2	r1i1p1f1
BCC-CSM2-MR	r1i1p1f1
CMCC-CM2-SR5	r1i1p1f1
EC-Earth3	r1i1p1f1, r3i1p1f1, r4i1p1f1
HadGEM3-GC31-LL	r1i1p1f3
HadGEM3-GC31-MM	r1i1p1f3
KIOST-ESM	r1i1p1f1
MIROC6	r1i1p1f1
MPI-ESM1-2-HR	r1i1p1f1, r2i1p1f1
MPI-ESM1-2-LR	r1i1p1f1
MRI-ESM2-0	r1i1p1f1

WBGT calculation

WBGT is not available as a routine meteorological measurement, so various approaches have been developed to approximate it. The simplified WBGT (Government of Australia, 2010) and Environment Stress Index (Moran, et al., 2001) (Moran, et al., 2003) represent two relatively simple *ad hoc* approximations, though are subject to potentially large biases out of the conditions under which they were developed (Grundstein & Cooper, 2018) (Havenith & Fiala, 2011). Here, we use a physically based model developed by Liljegren (2008) to directly simulate WBGT measurements. This model implements heat budget analyses on the sensors of WBGT measurement instruments, which leads to two equations for T_w and T_g (equations 9 and 17 in (Liljegren, 2008)). Liljegren's model has been extensively calibrated and validated (with a Root Mean Square difference of less than 1°C) and seen increasing applications in recent years (Takakura J. Y., et al., 2017) (Takakura J. , et al., 2018) (Casanueva, et al., 2020).

Kong and Huber (2021) developed a Python implementation of Liljegren's code (originally in FORTRAN and C language) that is especially suitable for processing climate model output and is used in this paper. WBGT is calculated under both outdoor and indoor conditions. For indoor conditions, solar radiation is set to zero and wind speed is fixed at 1 m/s. For the detailed calculation procedure, please refer to (Liljegren, 2008) and Kong and Huber (2021).

Bias correction

By quantifying labor loss as a function of global mean surface air temperature warming, we decouple our analysis from the time-path of forcing. This effectively reduces model spread and biases on climate sensitivity, and essentially removes the concern of 'when does warming happen?' and 'what scenario of emissions is being followed?', which are the dominant sources of uncertainty in a normal heat stress projection. Nevertheless, each climate model has different absolute climate states for the same baseline period and warming targets, which will introduce uncertainty to the quantification of labor productivity shock due to the nonlinearity of labor response. To further reduce this element of uncertainty, we perform bias correction on climate models based on ERA5 reanalysis data.[7] First, WBGT anomalies are calculated at 3-hourly frequency between the average year of the baseline period and the 3°C warming world, for each Global Climate Model. Second, the WBGT anomaly field is downscaled to ERA5 resolution and then added to ERA5 reanalysis data (which is resampled to 3-hourly frequency) of each year from 1961-1990. Finally, labor productivity shock is assessed by comparing the ERA5 baseline and ERA5 baseline adding anomalies from each climate model. By adopting a common baseline from ERA5 reanalysis, we expect to have more realistic estimates of labor productivity shock with lower uncertainty.

Estimation of Labor Capacity Losses by Sector and Labor Type

Formally, using data heat stress/WBGT projection and labor response functions described in the main text, we obtain $z_{r,g}^{i,c}$- the percentage decline in labor capacity in grid cell g (in region r) for work intensity i, where $i = \{200\ \mathrm{W}, 300\ \mathrm{W}, 400\ \mathrm{W}, 600\ \mathrm{W}\}$ performed in indoor or outdoor conditions indicated by the index c, where $c = \{in, out\}$ under heat stress levels consistent with 3°C mean global warming.

Next, the shock at each grid cell is calculated considering the work intensity and outdoor exposure of each labor category in each economic activity within the grid cell. This allows for a more accurate estimate of labor productivity shock for use in our economic framework. That is, we estimate:

[7] ERA5 is the fifth-generation atmospheric reanalysis of the global climate covering the period from January 1950 to present. ERA5 is produced by the Copernicus Climate Change Service at the European Centre for Medium-Range Weather Forecasts.

$$z_{l,a,r,g} = \sum_{c} \sum_{i} z_{r,g}^{i,c} \alpha_{l,a}^{c} \beta_{l,a}^{i} \quad (4)$$

where,

$$\sum_{c} \alpha_{l,a}^{i} = 1 \quad (5)$$

$$\sum_{i} \beta_{l,a}^{c} = 1 \quad (6)$$

Here, $\beta_{l,a}^{c}$ is the portion of labor type l in activity a exposed to $c = \{in, out\}$, and $\alpha_{l,a}^{i}$is the portion of labor of labor type l in activity a with a work intensity of $i = \{200\ \mathrm{W}, 300\ \mathrm{W}, 400\ \mathrm{W}, 600\ \mathrm{W}\}$. The information on α and β are obtained from the U.S. BLS Occupational Requirements Survey (ORS).[8] The ORS provides job-related information regarding physical demands and environmental conditions, including data related to work intensity and outdoor exposure, for different occupations and economic sectors (BLS, 2020). That is, work intensity is described in terms such as 'sedentary' to 'very heavy work'. We map these descriptors to specific assumption about metabolic output (e.g., we assume 'very heavy work' is equivalent to a metabolic output of 600W) and specific data about the proportion of work done outdoors. These assumptions are listed in Table 5.

Table 5: Occupation-required strength to working rate:

BLS Intensity Descriptor	Assumed Metabolic Rate
Sedentary	0
Light work	200 W
Medium work	300 W
Heavy work	400 W
Very heavy work	600 W

We organized BLS occupations into 22 categories in 13 sectors. We further categorized these 22 occupations into four labor types (white collar, blue-collar, pink, and purple) while the 13 BLS activities were aggregated into seven broad sectors (agriculture, extraction, construction, manufacturing, trade, transport, and services).

Finally, we aggregate over grid cells to obtain two different sets of region-level losses: (i) we aggregate the labor shock that applies to non-agricultural sectors using gridded population (pop) as weights, assuming non-agricultural activities follow the spatial pattern of population, and (ii) we aggregate the

[8] These data pertaining to the U.S. are applied to all regions, thus assuming that work profiles (strength requirement and outdoor exposure) for different occupations in different regions are not significantly different from the U.S. This is a strong assumption but is the best available information.

labor shock for agricultural sectors using gridded values of crop production (val) as weights, assuming agricultural activities follow the spatial pattern of crop production. That is,

$$z_{l,a_1,r} = \sum_{g \in r} \frac{pop_{r,g}}{pop_r} z_{l,a_1,r,g} \quad (2)$$

$$z_{l,a_2,r} = \sum_{g \in r} \frac{val_{r,g}}{val_r} z_{l,a_2,r,g} \quad (3)$$

where labor capacity losses $z_{l,a_1,r}$obtained from equation (2) are applied to non-agricultural sectors and $z_{l,a_2,r}$obtained from equation (3) are applied to agricultural sectors.

Economic Model and Database

We use GTAP-POV; an extension of the GTAP model (Hertel, 1997) (Corong, Hertel, McDougall, Tsigas, & van der Mensbrugghe, The standard GTAP model, version 7., 2017). It is a macro-to-micro approach where macro changes from the main ('macro') model are fed into a micro-simulation HH model to calculate poverty impacts using an elasticity approach. For this study, we paired GTAP-POV with data from version 10 of the GTAP database (Aguiar, Chepeliev, Corong, McDougall, & van der Mensbrugghe, 2019). GTAP-POV groups all HHs in the national surveys into seven different strata based on income sources. The poverty headcount data were updated to reflect most recently available information available from the World Bank World Development Indicators. Changes in the poverty headcount by stratum are driven by changes in real income of the poor as well as the elasticity of poverty with respect to changes in income. The former depends on the earnings shares and the real cost of living at the poverty line. The latter depends on the density of the stratum population around the poverty line.

Annex 2: Additional Figures and Tables

Figure 23: Composition of Ghana's Value-Added in the base

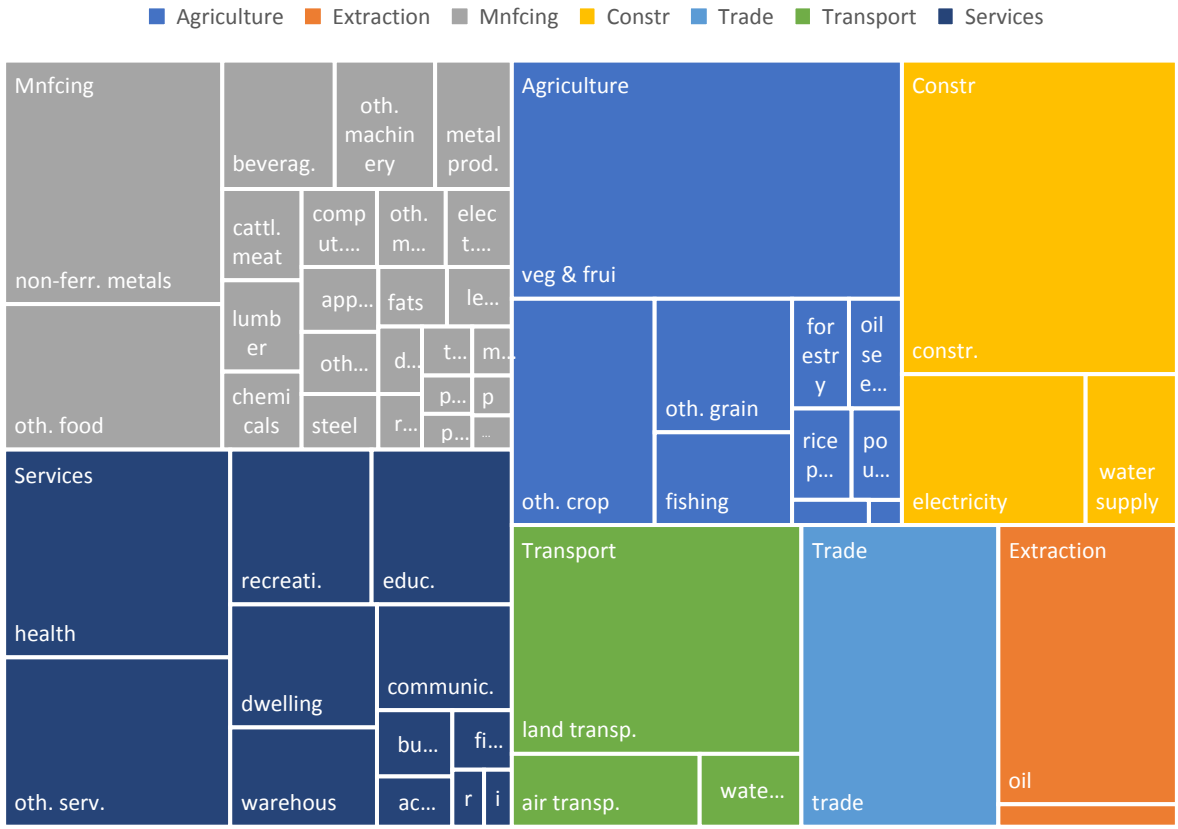

Table 6: $WBGT_{eff}$ reference values for acclimatized and unacclimatized people for five classes of metabolic rate

Metabolic Rate Class	**Metabolic Rate** (Watts)	**WBGT reference limit for persons acclimatized to heat**	**WBGT reference limit for persons unacclimatized to heat**
Class 0: Resting metabolic rate	115 W	33°C	32°C
Class 1: Low metabolic rate	180 W	30°C	29°C
Class 2: Moderate metabolic rate	300 W	28°C	26°C
Class 3: High metabolic rate	415 W	26°C	23°C
Class 4: Very high metabolic rate	520 W	25°C	20°C

Source: (ISO, 2017)

Annex 3: Bibliography

Aguiar, A., Chepeliev, M., Corong, E., McDougall, R., & van der Mensbrugghe, D. (2019). The GTAP Data Base: Version 10. *Journal of Global Economic Analysis, 4*(1), 1-27.

BLS. (2020). *The Occupational Requirements Survey (ORS).* Washington, D.C.: Bureau of Labor Statistics (BLS).

Brode, P., Fiala, D., Lemke, B., & Kjellstrom, T. (2018). Estimated work ability in warm outdoor environments depends on the chosen heat stress assessment metric. *International Journal of Biometeorology*, 62(3), 331–345.

Casanueva, A., Kotlarski, S., Fischer, A., Flouris, A., Kjellstrom, T., Lemke, B., . . . & Liniger, M. (2020). Escalating environmental summer heat exposure—a future threat for the European workforce. *Regional Environmental Change, 20*(2), 1-14.

Colmer, J. (2021). Temperature, Labor Reallocation, and Industrial Production:. *American Economic Journal: Applied Economics*, 13(4): 101–124.

Corong, E. L., Hertel, T. W., McDougall, R., Tsigas, M. E., & van der Mensbrugghe, D. (2017). The standard GTAP model, version 7. *Journal of Global Economic Analysis, 2*(1), 1-119.

Corong, E. L., Hertel, T. W., McDougall, R., Tsigas, M. E., & van der Mensbrugghe, D. (2017). The standard GTAP model, version 7. *Journal of Global Economic Analysis, 2*(1), 1-119.

de Lima, C. Z., Buzan, J. R., Moore, F. C., Baldos, C. U., Huber, M., & Hertel , T. W. (2021). Heat stress on agricultural workers exacerbates crop impacts of climate change. *Environmental Research Letters, 16*(4), 044020.

Ghana Statistical Service. (2017). *Ghana Living Standard Survey 7.* Retrieved from https://statsghana.gov.gh/mediacentre_newsdetails.php?statsnews=MzY5NDc5ODg1LjI3MQ==/statsnews/238922onno

Government of Australia. (2010, 2 5). *Bureau of Meteorology*. Retrieved from Thermal Comfort observations: http://www.bom.gov.au/info/thermal_stress/#approximation

Grundstein, A., & Cooper, E. (2018). Assessment of the Australian Bureau of Meteorology wet bulb globe temperature model using weather station data. *International journal of biometeorology, 62*(12), 2205-2213.

Havenith, G., & Fiala, D. (2011). Thermal indices and thermophysiological modeling for heat stress. *Comprehensive Physiology, 6*(1), 255-302.

Hertel, T. W. (1997). *Global trade analysis: modeling and applications.* Cambridge University Press.

Hsiang, S. (2021, September 30). *Presentation: "Labor supply in a wamer world: The impact of climate change on the global workforce.".* Retrieved from https://www.frbsf.org/: https://www.frbsf.org/economic-research/events/2019/november/economics-of-climate-change/labor-supply-in-a-warmer-world/

IPCC. (2014). *Climate Change 2014: Impacts, Adaptation, and Vulnerability. (Chapter 2).* New York: Intergovernmental Panel on Climate Change. Cambridge University Press.

ISO. (2017). *Ergonomics of the thermal environment — Assessment of heat stress using the WBGT index.* Geneva: International Organization for Standardization (ISO).

Key, N., & Sneeringer, S. (2014). Potential Effects of Climate Change on the Productivity of U.S. Dairies. *American Journal of Agricultural Economics*, 96 (4): 1136-56.

Liljegren, J. C. (2008). Modeling the wet bulb globe temperature using standard meteorological measurements. *Journal of occupational and environmental hygiene*, 5(10), 645-655.

Mader, T. L. (2014). Animal Welfare Concerns for Cattle Exposed to Adverse Environmental Conditions . *Journal of Animal Science*, 92 (12): 5319–24.

Moran, D. S., Pandolf, K. B., Laor, A., Heled, Y., Matthew, W. T., & Gonzalez, R. R. (2003). Evaluation and refinement of the environmental stress index for different climatic conditions. *Journal of basic and clinical physiology and pharmacology, 14*(1), 1-16.

Moran, D. S., Pandolf, K. B., Shapiro, Y., Heled, Y., Shani, Y., Mathew, W. T., & Gonzalez, R. R. (2001). An environmental stress index (ESI) as a substitute for the wet bulb globe temperature (WBGT). . *Journal of thermal biology, 26*(4-5), 427-431.

Patz, J., Frumkin, H., Holloway, T., Vimont, D., & Haines, A. (2014). Climate Change: Challenges and Opportunities for Global Health. *Journal of the American Medical Association*, 312 (15): 1565–80.

Saeed, W., Haqiqi, I., Kong, Q., Huber, M., Buzan, J., & Hertel, T. (2021). Labor Heat Stress under a Warming Climate Increases Poverty across the Tropics.

Takakura, J. Y., Fujimori, S., Takahashi, K., Hijioka, Y., Hasegawa, T., Honda, Y., & & Masui, T. (2017). Cost of preventing workplace heat-related illness through worker breaks and the benefit of climate-change mitigation. *Environmental Research Letters, 12*(6), 064010.

Takakura, J., Fujimori, S., Takahashi, K., Hasegawa, T., Honda, Y., Hanasaki, N., . . . Masui, T. (2018). Earth's Future. *Limited Role of Working Time Shift in Offsetting the Increasing Occupational-Health Cost of Heat Exposure, 6*, 1588-1602.

Yu, C. H. (2014). Case Studies on the Effects of Climate Change on Water, Livestock and Hurricanes. *PhD Dissertation, Texas A&M University*.